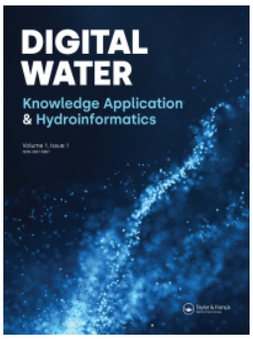

Taylor & Francis
Taylor & Francis Group

Digital Water

Knowledge Application & Hydroinformatics

ISSN: 2837-5807 (Online) Journal homepage: www.tandfonline.com/journals/tdwa20

A novel WDN pipe replacement prioritisation methodology and software

Panagiotis Dimas , Nikos Pelekanos , Georgios Moraitis , Archontia Lykou , Spyridon Tsattalios , George Karavokiros , Christodoulos Pantazis , Panagiotis Kossieris , Andreas Efstratiadis & Christos Makropoulos

To cite this article: Panagiotis Dimas , Nikos Pelekanos , Georgios Moraitis , Archontia Lykou , Spyridon Tsattalios , George Karavokiros , Christodoulos Pantazis , Panagiotis Kossieris , Andreas Efstratiadis & Christos Makropoulos (2026) A novel WDN pipe replacement prioritisation methodology and software, Digital Water, 4:1, 2724253, DOI: 10.1080/28375807.2026.2724253

To link to this article: https://doi.org/10.1080/28375807.2026.2724253

© 2026 The Author(s). Published by Informa UK Limited, trading as Taylor & Francis Group.

Published online: 26 Aug 2026.

Submit your article to this journal

View related articles

View Crossmark data

Full Terms & Conditions of access and use can be found at
https://www.tandfonline.com/action/journalInformation?journalCode=tdwa20

DIGITAL WATER
2026, VOL. 4, NO. 1, 2724253
https://doi.org/10.1080/28375807.2026.2724253

Routledge
Taylor & Francis Group

RESEARCH ARTICLE

OPEN ACCESS Check for updates

A novel WDN pipe replacement prioritisation methodology and software

Panagiotis Dimas, Nikos Pelekanos, Georgios Moraitis, Archontia Lykou, Spyridon Tsattalios, George Karavokiros, Christodoulos Pantazis, Panagiotis Kossieris, Andreas Efstratiadis and Christos Makropoulos

Department of Water Resources and Environmental Engineering, School of Civil Engineering, National Technical University of Athens, Athens, Greece

ABSTRACT

This paper presents a methodological framework for optimising pipe replacement in urban water distribution networks (WDNs). The approach combines resilience-based network analysis, historical failure records, spatial clustering and life-cycle cost (LCC) optimisation within a decision support environment. Graph-theoretic indicators of topological importance are merged with failure data to produce a composite vulnerability index, while spatial autocorrelation methods highlight clusters of recurring bursts and increased topological significance. LCC optimisation then determines cost-effective replacement horizons, smoothing annual investments under budget constraints. The outcomes are consolidated into contract-ready groups of continuous pipes, enabling direct translation into renewal schedules. A pilot application showed the framework's ability to identify critical mains, optimise intervention timing and improve cost-effectiveness compared with traditional age-based strategies.

ARTICLE HISTORY
Received 28 July 2026
Accepted 7 August 2026

1. Introduction

Water distribution networks (WDNs) constitute one of the most extensive and capital-intensive asset categories for urban water utilities (Engelhardt *et al.* 2000). As networks expand and age, buried pipelines progressively deteriorate, resulting in increased leakage, Non-Revenue Water (NRW), service disruptions and escalating repair costs. These challenges are particularly pronounced in older European cities, where large parts of the network were constructed several decades ago using materials that are now more vulnerable under present operating conditions. In Athens, for example, the average pipe age is close to fifty years, while extensive sections of asbestos cement and cast-iron mains are known to exhibit recurrent failures, aggravated by high operational pressures and rapidly evolving consumption patterns.

Traditional rehabilitation policies, such as age-based replacement or approaches that rely exclusively on expert judgement, are increasingly inadequate. They overlook differences in network topology, localised patterns of failure, and the long-term economic trade-offs between repair and replacement. At the same time, utilities seek transparent, defensible and evidence-based asset management strategies that can be operationalised within real-world financial and operational constraints.

The present study introduces an integrated methodology for prioritising pipe replacement in WDNs. The methodology combines resilience-based network analysis (Klise *et al.* 2018), empirical failure data, spatial clustering techniques, life-cycle cost (*LCC*) optimisation (Hasegawa *et al.* 2018, Ghobadi *et al.* 2021) and the formation of contract-ready replacement groups within a GIS-based Decision Support System (DSS). A pilot implementation in a pressure zone of the Athens WDN is presented to demonstrate the applicability and advantages of the method relative to conventional age-based strategies.

CONTACT Panagiotis Dimas pdimas@mail.ntua.gr Department of Water Resources and Environmental Engineering, School of Civil Engineering, National Technical University of Athens, 9 Iroon Polytechniou str., Athens 15772, Greece

© 2026 The Author(s). Published by Informa UK Limited, trading as Taylor & Francis Group.
This is an Open Access article distributed under the terms of the Creative Commons Attribution-NonCommercial License (http://creativecommons.org/licenses/by-nc/4.0/), which permits unrestricted non-commercial use, distribution, and reproduction in any medium, provided the original work is properly cited. The terms on which this article has been published allow the posting of the Accepted Manuscript in a repository by the author(s) or with their consent.

2. Materials and methods

The methodological framework transforms raw network and failure data into optimised and construction-ready investment plans through five components. These components are: *(i)* topological resilience analysis, *(ii)* construction of a composite failure index, *(iii)* spatial clustering of vulnerable areas, *(iv)* life-cycle cost optimisation, and *(v)* grouping of pipes into contract-ready renewal segments.

2.1. Topological resilience analysis

In the first component the WDN is represented as an undirected graph, with pipes as edges and junctions as nodes. This representation enables the computation of graph-theoretic indicators that quantify the structural importance of each pipe independently of hydraulic modelling. Three indicators are employed: Betweenness Centrality, Closeness Centrality and the identification of Bridges.

Betweenness Centrality (BC) measures how frequently a pipe lies on the shortest paths between pairs of nodes. Pipes with high BC are critical for maintaining connectivity, as their failure can significantly affect the ability of the network to route flows. Closeness Centrality (CC) expresses the inverse of the average shortest path length from a node (or associated pipe) to all other nodes and thus reflects its centrality in terms of path efficiency. Bridges (B) are edges whose removal increases the number of connected components of the graph, directly indicating structural vulnerability.

All three indicators are first normalised to the $[0, 1]$ interval, yielding the normalised metrics $\widetilde{BC}_i$, $\widetilde{CC}_i$ and $\tilde{B}_i$ for each pipe, i. These are then combined into a single resilience-based importance score R_i according to:

$$R_i = \frac{w_{BC}\widetilde{BC}_i + w_{CC}\widetilde{CC}_i + w_B\tilde{B}_i}{w_{BC} + w_{CC} + w_B} \tag{1}$$

where w_{BC}, w_{CC} and w_B are non-negative weights that can be selected in cooperation with utility experts. In the pilot application, equal weights were used, so that each indicator contributed equally to the composite resilience score, R_i. This index allows the identification of structurally important mains that warrant particular attention in the subsequent prioritisation stages.

2.2. Composite failure index

The second component introduces empirical performance data. Historical records of pipe failures are collected from the utility's GIS database, customer service logs and maintenance management systems. For each pipe i, the failure frequency is normalised to give a failure rate indicator, F_i. This prevents bias towards specific pipes and reflects the underlying deterioration behaviour more consistently.

To integrate structural importance and empirical fragility into a single prioritisation metric, the methodology defines a Composite Failure Index, CFI_i. The latter combines the resilience score, R_i, with the normalised failure rate, F_i, using a convex combination:

$$CFI_i = \alpha R_i + (1 - \alpha)F_i \tag{2}$$

where $0 \leq \alpha \leq 1$ is a weighting factor. When α is large, more emphasis is placed on topological importance, whereas smaller values emphasise historical performance data. In the pilot study, a value of $\alpha = 0.5$ is selected to give equal weight to both components, following consultation with the utility's engineers.

The Composite Failure Index, as defined in Equation (2), highlights pipes that are simultaneously crucial for connectivity and prone to recurrent bursts. It provides a flexible mechanism to incorporate both structural and operational knowledge into a unified measure of vulnerability.

2.3. Spatial clustering analysis

2.3.1. Global Moran's I index

Having computed the Composite Failure Index that combines topological criteria and failure counts, the study area is divided into a rectangular grid of resolution $\Delta x \times \Delta x$. The cell size of the grid is a parameter to be optimised, as will be discussed later. Each grid cell represents a geographical entity with specific

characteristics in terms of topological indicators and number of failures, and it contains a sub-group of the pipes belonging to the network of the study area.

Next, to determine whether spatial correlation exists among the different cells of the grid, Moran's I index is employed. In statistics, Moran's I is a measure of spatial autocorrelation, which refers to the correlation of a signal between neighbouring locations in space. It is more complex than one-dimensional autocorrelation because it pertains to two- or three-dimensional space and involves multiple directions.

If x_i denotes the attribute value (for example, failure density or Composite Failure Index) of pipe i, and w_{ij} denotes the spatial weight between pipes i and j, Moran's I statistic is given by:

$$\mathrm{I} = \frac{N}{W}\frac{\sum_{i=1}^{N}\sum_{j=1}^{N} w_{ij}(x_i-\bar{x})(x_j-\bar{x})}{\sum_{i=1}^{N}(x_i-\bar{x})^2} \tag{3}$$

where N is the number of spatial units (cells of the rectangular grid in our case), $\bar{x}$ is the mean of the attribute, and $W = \sum_{i=1}^{N}\sum_{j=1}^{N} w_{ij}$ is the sum of all spatial weights. Positive and statistically significant values of Moran's I indicate clustering of similar values, whereas negative values indicate spatial dispersion (see Figure 1).

Within the framework of the methodology presented in this work, Moran's I index, the $z-score$ and the $p-value$ (significance level) are calculated for different grid-cell dimensions Δx. Ultimately, the selected grid size is the one that maximises Moran's I, while simultaneously yielding a positive $z-score$ ($z-score>0$) and a $p-value$ corresponding to a confidence level of at least 95% ($p-value<0.05$).

2.3.2. Local indicators of spatial association (LISA) analysis and clustering

The global analysis of spatial autocorrelation using Moran's global I index provides only a single statistic summarising the behaviour of the entire study area. In other words, global analysis assumes spatial homogeneity. If this assumption does not hold, then a single global statistic becomes meaningless, as the underlying spatial processes may vary across the study area.

Moreover, even when global autocorrelation or clustering is weak or absent, it is still possible to identify localised clusters through local spatial autocorrelation analysis. The fact that Moran's I is the sum of individual cross-products is exploited by the "Local Indicators of Spatial Association" (LISA), which perform clustering at the level of individual spatial units by computing a local Moran's I value for each unit and evaluating its statistical significance. Starting from the formulation of the global index, the local Moran's I for each spatial unit I can be derived as:

$$\mathrm{I}_i = \frac{x_i-\bar{x}}{m_2}\sum_{j=1}^{N} w_{ij}(x_j-\bar{x}) \tag{4}$$

where

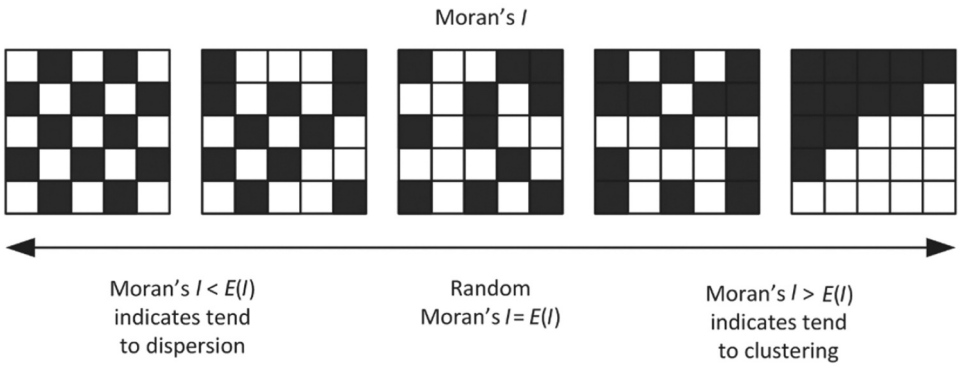

Figure 1. Global Moran's I and spatial autocorrelation source (Grekousis, 2020).

$$m_2 = \frac{\sum_{i=1}^{N} (x_i - \bar{x})^2}{N} \tag{5}$$

is the second central moment of the distribution. The global Moran's I can then be expressed as the average of the local indices,

$$\mathrm{I} = \frac{\sum_{i=1}^{N} \mathrm{I}_i}{N} \tag{6}$$

While global spatial autocorrelation can demonstrate the presence of clustering or a positive spatial association between the values of a variable and those of its neighbours, it does not indicate where clusters are located. This is precisely the role of local spatial autocorrelation, obtained through LISA analysis. In general, the interpretation of the local Moran's I values is as follows: negative values indicate that neighbouring units are dissimilar or spatially dispersed (for example, High–Low or Low–High relationships). Neutral values indicate an absence of meaningful association or a random spatial pattern. Positive values indicate that neighbouring units are similar or spatially concentrated (for example, High–High or Low–Low relationships).

LISA analysis uses the local Moran's I values to detect clusters in specific areas of the map and to classify them into five types:

(i) *High–High (HH)*, where a high-value location is surrounded by neighbours that also have high values,
(ii) *Low–Low (LL)*, where a low-value location is surrounded by low-value neighbours,
(iii) *Low–High (LH)*, where a low-value location is surrounded by high-value neighbours,
(iv) *High–Low (HL)*, where a high-value location is surrounded by low-value neighbours,
(v) *Non-significant (NS)*, where no statistically significant spatial pattern is detected.

The High–High (*HH*) and Low–Low (*LL*) categories correspond to positive spatial autocorrelation, whereas the High–Low (*HL*) and Low–High (*LH*) categories correspond to negative spatial autocorrelation.

Once the LISA analysis has been completed for the grid size determined in the previous stage, the clusters of grid cells are available for further processing. The grid cells are then classified according to the cluster type to which they belong and their standardised number of failures. The prioritisation begins with the *HH* cell with the highest number of failures and proceeds with the *HL*, *LH* and *LL* cells, respectively. In this way, an *initial prioritisation programme* is established, in which each grid cell represents a sub-zone of network pipes designated for replacement.

2.4. Life-cycle cost (LCC) optimization

2.4.1. Setting the scene

The life-cycle cost (*LCC*) of a pipeline is defined as the sum of all expenditures associated with it over its entire service life, including acquisition, maintenance, replacement, repair and disposal at the end of its operational period. In the present methodology, *LCC* is computed as:

$$LCC(D,t) = CI(D,t) + CR(D,t) \tag{7}$$

where *CI* is the initial cost (€/km/year), *CR* is the recurrent cost (€/km/year), *D* is the pipe diameter (mm) and *t* is the time elapsed since the pipe's installation or replacement (in years). The term *CI* includes only the annualised replacement cost of the pipe (depreciation), while *CR* includes only the annual repair cost. Assuming the simplest form of linear depreciation of the asset value, the initial cost is calculated as:

$$CI(D,t) = \frac{CP(D)}{t} \tag{8}$$

where *CP* is the replacement cost of the pipe (€/km). The recurrent cost *CR* is the product of the unit repair cost and the average failure rate within the replacement interval, and is therefore expressed as:

$$CR(D,t) = Cr(D) \times \frac{\sum_{A=1}^{t} Fr(D,A)}{t} \tag{9}$$

where Cr is the repair cost per failure (€/failure). This can be estimated using the empirical relationship proposed by the US Army Corps of Engineers (Kim and Mays 1990), which depends solely on diameter:

$$Cr(D) = 1.300\left(\frac{D}{304.8}\right)^{0.62} \times 800 \tag{10}$$

The failure rate Fr(failures/km/year) depends on pipe diameter, age A, material and other parameters. It can be expressed through the empirical relationship (Shin *et al.* 2016):

$$Fr(D,A) = 0.109 \times e^{-0.0064D} \times (A)^{1.377} \tag{11}$$

To accurately estimate failure rates, actual network failure records must be used to calibrate empirical relationships of this form through appropriate statistical analysis. Figure 2 (left) illustrates an example of an *LCC* curve. As the age of a pipe increases, the recurrent cost rises while the initial cost decreases. Summing the two yields the total cost. The minimum point of the total cost curve corresponds to the optimal replacement time t^*, which represents the economic service life of the pipe. The minimum *LCC* value (*LeastLifeCycleCost* − *LLCC*) is defined as the *LCC* associated with t^*.

If the *LCC* values of individual pipes are aggregated at the network or sub-network level, the total *LCC* of the system is obtained:

$$LLCC_N = \sum_{i=1}^{n} LCC\left(D_i, t_i^*\right) \times L_i \tag{12}$$

where n is the number of pipes and L_i is the length of pipe i. The *LCC* of each pipe is calculated to determine its optimal replacement time. However, if the annual costs for all pipes are summed directly, the resulting investment time series exhibits large year-to-year fluctuations and high volatility, making the investment plan impractical and difficult to implement. For this reason, to smooth the investment time series, a time window is defined around the optimal replacement year t^* within which the pipe replacement is allowed to occur (see Figure 2 on the right).

2.4.2. Defining the optimisation problem

Considering the analyses of the previous sections, the optimisation problem can now be formulated as follows. The decision variable of the problem is a vector $[t_1, t_2, t_3, \ldots, t_n]$ containing the replacement times of the individual pipes of the network or its sub-set. The objective functions of the problem concern the minimisation of the *LCC* of the network (i.e. the difference between LCC_N and $LLCC_N$), as well as the minimisation of the second derivative of the time series of annual investments in order to make it as smooth as possible, and are formulated as follows:

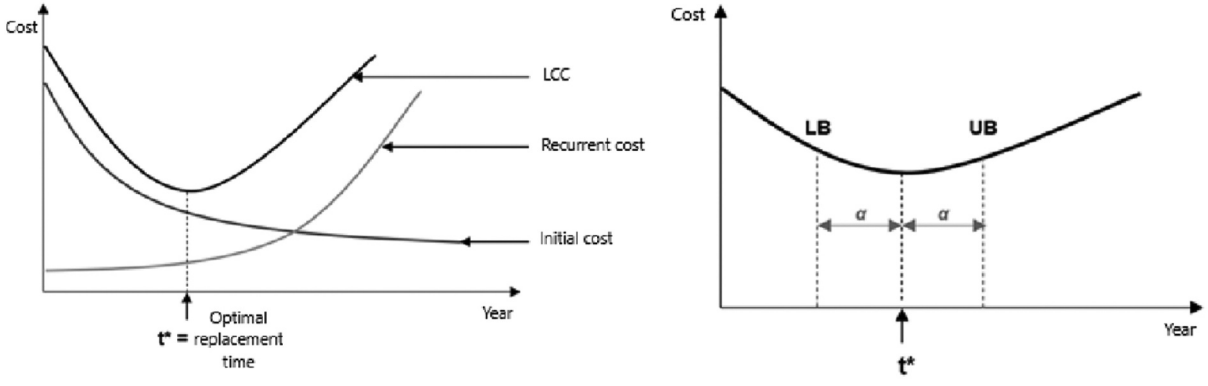

Figure 2. LCC curve for a single pipe (left), and definition of a time window within the pipe replacement is allowed to occur (right).

$$Minf_1(t_1,\ldots,t_n) = \left[\sum_{i=1}^{n} LCC(D_i,t_i)\times L_i\right] - LLCC_N \tag{13}$$

$$Minf_2(t_1,\ldots,t_n) = \sum_{t=1}^{t_{span}} \left(\frac{d^2 I_y^t}{dt^2}\right)^2 \tag{14}$$

where I_y^t is the time series of investment and n is the number of pipes in the problem.

The constraints of the problem concern the non-exceeding of the interval $(t^* \pm a)$ within which the replacement of the pipes is allowed. In total, the optimisation problem is formulated as follows:

$$Min\{f_1(t_1,\ldots,t_n), f_2(t_1,\ldots,t_n)\} \tag{15}$$

subject to the constraint: $\{t_i^* - a \le t_i \le t_i^* + a\}$, where a is the parameter that determines the allowed relaxation interval of the optimal replacement time of each pipe. Since the solution to the optimisation problem as formulated above leads to a Pareto front of different solutions, we cannot judge which is the best solution in an objective way. The knee point is the solution on the Pareto front with the maximum marginal utility, which is considered as the preferred solution if there is no other preference. It is the best compromise between the two criteria, since there is no auxiliary information.

2.5. Grouping pipes into contract-ready renewal segments

The final step of the methodological framework concerns the identification of *pipe groups* which constitute continuous sections of the network and can potentially also constitute continuous sections of replacement contracts. In contrast to the previous steps of the methodology, the last part functions more as an auxiliary tool for supporting and visualising the results, while no computational and statistical models are performed, but simply aggregated data are displayed. From the study area, and given the desired replacement times of each pipe, the utility engineer selects a sub-group (set) of the study area that is of particular interest to him (e.g. pipes with a desired replacement time of 1–3 years, pipes made of asbestos cement, etc.).

The selected subgroup includes pipes scattered in the study area (as long as the user has not deliberately selected pipes that are in a connection sequence as a subgroup) and it is not necessary that they are all connected to each other but are in different random or even isolated sections. The auxiliary tool comes to supplement information on how many and which continuous sections of pipes (groups) of the network this subgroup consists of, by providing details such as *(i)* Coding of continuous sections, *(ii)* Sum of lengths of each continuous section, *(iii)* Weighted average value (by length) of the desired replacement year of each continuous section, and *(iv)* Logical condition (True/False) if each continuous section exceeds a minimum length (e.g. of contracting) that the utility engineer has defined.

3. Results and discussion

The proposed methodology was applied in a pilot sub-zone of the greater Athens WDN, located in the southern greater metropolitan area of Athens. The study area comprises a dense urban residential district supplied through a PRV-controlled main and characterised by ageing asbestos-cement distribution pipes. The broader zone includes approximately 54 km of distribution pipes, of which almost 80% are asbestos cement ones installed between the 1950s and 1990s. Historical repair records from the utility's failure notification system and the Water Supply Portal were compiled and spatially referenced, producing a unified failure dataset for the entire pressure zone.

3.1. Topological resilience and composite vulnerability patterns

The topological analysis (*Step 1*) highlighted structurally sensitive parts of the sub-zone. High *BC* values were associated with centrally positioned distribution links forming small but critical bridges between local loops. *CC* revealed a set of centrally accessible pipes acting as local distribution hubs, while the B indicator identified a limited but important set of edges whose removal would disconnect small residential blocks.

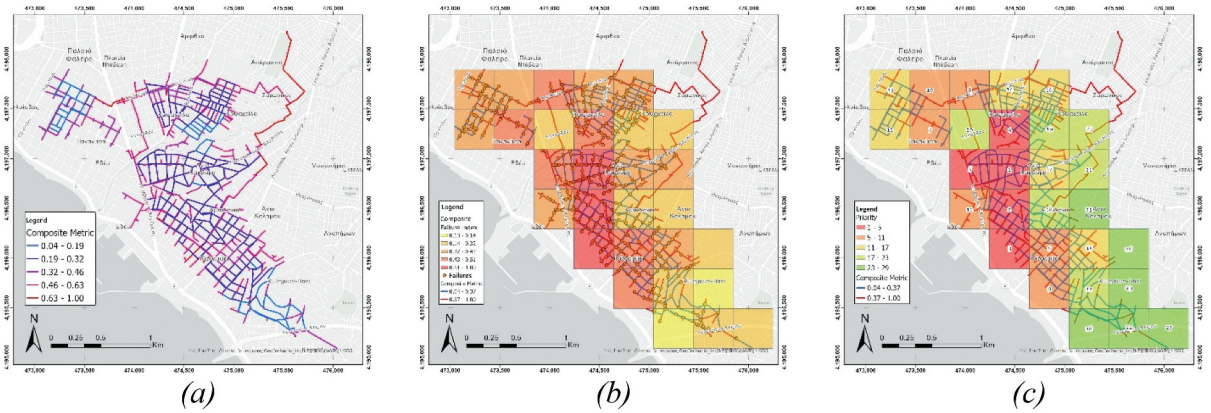

Figure 3. *(a)* Composite metric of topological resilience, *(b)* Composite failure index per grid cell, and *(c)* Grid cell prioritization.

These metrics were aggregated into the composite topological index (*CM*), producing a spatially coherent pattern of central and peripheral importance (Figure 3a).

In *Step 2*, *CM* was combined with the normalised failure density, and the resulting weighted index was projected onto a rectangular grid that served as the unit of spatial analysis. Several grid sizes (100–1000 m) were tested. Moran's *I*, the $z-score$ and the $p-value$ were computed for each configuration. The grid size of $\Delta x = 400$ m maximised Moran's *I* under statistically significant spatial autocorrelation ($p < 0.05$) and was therefore selected as the optimal grid resolution. At this scale, both failures and composite vulnerability formed distinct spatial clusters (Figure 3b).

LISA analysis revealed four populated cluster types: HH, HL, LH and LL. HH clusters were concentrated in the north-central part of the sub-zone, where aged asbestos-cement pipes and dense historical failure patterns overlap. These were followed by HL and LH cells, while LL cells were located in recently rehabilitated or hydraulically peripheral areas. Based on this classification, grid cells were automatically prioritised, beginning with the HH cell with the highest standardised failure rate (Figure 3c). This formed the initial geographic prioritisation schedule, with each high-priority cell representing a candidate replacement sub-area.

3.2. Life-cycle cost (LCC) analysis and optimal replacement timing

Step 3 applied the Life-Cycle Cost optimisation framework to the highest-priority grid cell. The selected cell contained 38 pipes of varying diameters, materials and installation years. For each pipe, the individual *LCC* curve was computed using the local repair rate information and the updated replacement cost structure. The shapes of the *LCC* curves were consistent with typical ageing profiles: increasing recurring repair costs and decreasing annualised replacement cost as age increases. The minimum *LCC* for each pipe yielded the unconstrained optimal replacement year t^*.

The unconstrained schedule produced extreme annual investment peaks, reflecting synchronised optimal replacement times. After applying the multi-objective optimisation (minimising both cumulative *LCC* and the second derivative of the investment time series), the replacement years were redistributed within the allowable window $t^* \pm \alpha$. The resulting smoothed schedule (see Figure 4c) significantly reduced volatility, producing a feasible annual investment profile without substantial deviation from the minimum *LCC*. This demonstrates the capability of the method to reduce unrealistic budget peaks while retaining cost-optimal decisions at the asset level.

3.3. Formation of contract-ready groups

In *Step 4* the optimised schedule was used to construct contract-ready pipe groups. For the pilot test, the sub-set of pipes with optimised replacement years in the 1–3 year range (38 pipes) was analysed. Despite being spatially non-continuous at the individual pipe level, the grouping algorithm successfully identified

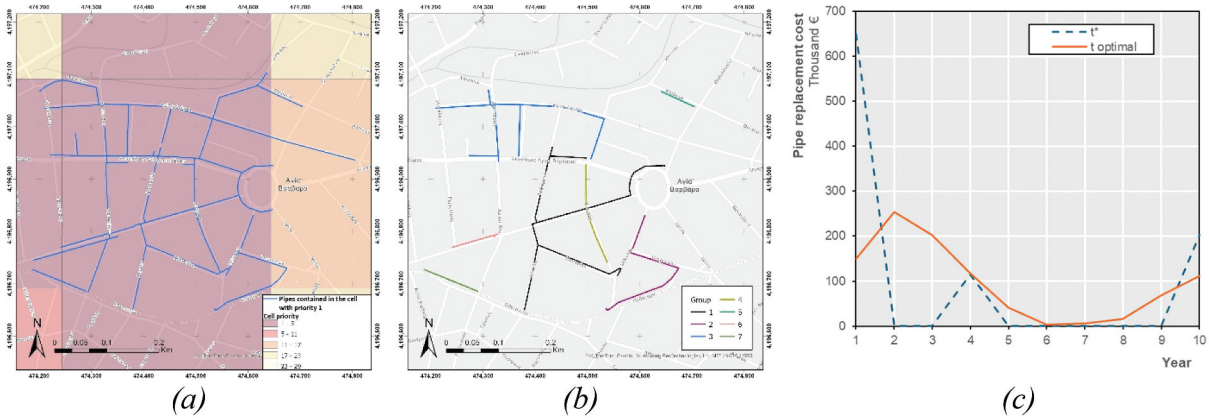

Figure 4. *(a)* Pipe sub-set contained in the cell with priority 1, *(b)* Continuous pipe segments suitable for construction tendering, and *(c)* Initial vs smoothened investment series.

seven continuous pipe segments. These ranged in length from 69 m to 877 m, with six of the seven exceeding the minimum practical length threshold of 70 m. Overall, 2318 m of pipeline-representing 97.1% of the whole selected subset-were consolidated into continuous segments suitable for construction tendering (Figure 4a,b).

4. Conclusions

This paper presented an integrated methodology and accompanying software for prioritising pipe replacement in WDNs. By coupling topological resilience indicators with normalised historical failure records and spatial clustering analysis, the approach delivers a robust assessment of pipe vulnerability. The subsequent life-cycle cost optimisation balances the cost of repairs and renewal, while an additional smoothing objective function controls the variability of annual investments. The final step, which groups pipes into coherent contract-ready segments, ensures that the methodology is directly applicable in water utility workflows and can be readily embedded into existing asset management processes.

Author contributions

CRediT: **Panagiotis Dimas:** Conceptualization, Data curation, Formal analysis, Funding acquisition, Investigation, Methodology, Project administration, Resources, Software, Supervision, Validation, Visualization, Writing – original draft, Writing – review & editing; **Nikos Pelekanos:** Conceptualization, Data curation, Formal analysis, Funding acquisition, Investigation, Methodology, Project administration, Resources, Software, Supervision, Validation, Visualization, Writing – original draft, Writing – review & editing; **Georgios Moraitis:** Conceptualization, Data curation, Formal analysis, Funding acquisition, Investigation, Methodology, Project administration, Resources, Software, Supervision, Validation, Visualization, Writing – original draft, Writing – review & editing; **Archontia Lykou:** Conceptualization, Data curation, Formal analysis, Funding acquisition, Investigation, Methodology, Project administration, Resources, Software, Supervision, Validation, Visualization, Writing – original draft, Writing – review & editing; **Spyridon Tsattalios:** Conceptualization, Data curation, Formal analysis, Funding acquisition, Investigation, Methodology, Project administration, Resources, Software, Supervision, Validation, Visualization, Writing – original draft, Writing – review & editing; **George Karavokiros:** Conceptualization, Data curation, Formal analysis, Funding acquisition, Investigation, Methodology, Project administration, Resources, Software, Supervision, Validation, Visualization, Writing – original draft, Writing – review & editing; **Christodoulos Pantazis:** Conceptualization, Data curation, Formal analysis, Funding acquisition, Investigation, Methodology, Project administration, Resources, Software, Supervision, Validation, Visualization, Writing – original draft, Writing – review & editing; **Panagiotis Kossieris:** Conceptualization, Data curation, Formal analysis, Funding acquisition, Investigation, Methodology, Project administration, Resources, Software, Supervision, Validation, Visualization, Writing – original draft, Writing – review & editing; **Andreas Efstratiadis:** Conceptualization, Data curation, Formal analysis, Funding acquisition, Investigation, Methodology, Project administration, Resources, Software, Supervision, Validation, Visualization, Writing – original draft, Writing – review & editing; **Christos Makropoulos:** Conceptualization, Data curation, Formal analysis, Funding acquisition, Investigation, Methodology, Project administration, Resources, Software, Supervision, Validation, Visualization, Writing – original draft, Writing – review & editing.

Disclosure statement

No potential conflict of interest was reported by the author(s).

Data availability statement

The data that support the findings of this study are available from the corresponding author upon reasonable request.

References

Engelhardt, M.O., Skipworth, P.J., Savic, D.A., Saul, A.J., and Walters, G.A., June 2000. Rehabilitation strategies for water distribution networks: a literature review with a UK perspective. *Urban water*, 2 (2), 153–170. doi:10.1016/S1462-0758(00)00053-4.

Ghobadi, F., Jeong, G., and Kang, D., 2021. Water pipe replacement scheduling based on life cycle cost assessment and optimization algorithm. *Water*, 13 (5), 605. doi:10.3390/w13050605.

2020. Spatial autocorrelation. *In*: Grekousis, G., ed. *Spatial analysis methods and practice: describe – explore – explain through GIS*. Cambridge: Cambridge University Press, 207–274. doi:10.1017/9781108614528.005.

Hasegawa, K., Arai, Y., and Koizumi, A., 2018. Life cycle cost-based pipe replacement Model and application in depopulation Scenario: (110). In: WDSA/CCWI Joint Conference Proceedings, Kingston, Ontario, Canada.

Kim, J.H. and Mays, L.W., Dec 1990. Rehabilitation and replacement of water distribution system components considering uncertainties. *Stochastic hydrology and hydraulics*, 4 (4), 277–294. doi:10.1007/BF01544082.

Klise, K.A., Murray, R., and Haxton, T., 2018. An overview of the water network tool for resilience (WNTR).

Shin, H., Joo, C., and Koo, J., Jan 2016. Optimal Rehabilitation model for water pipeline Systems with genetic algorithm. *Procedia engineering*, 154, 384–390. doi:10.1016/j.proeng.2016.07.497.